Coupling of the Subpolar Gyre and the Overturning Circulation During Abrupt Glacial Climate Transitions

M. Klockmann[1,2] , **U. Mikolajewicz[1]**, **H. Kleppin[3]**, and **J. Marotzke[1]**

[1]Max Planck Institute for Meteorology, Hamburg, Germany, [2]Institute of Coastal Research, Helmholtz-Zentrum Geesthacht, Geesthacht, Germany, [3]MARUM, Bremen, Germany

Abstract We present a mechanism for self-sustained ocean circulation changes that cause abrupt temperature changes over Greenland in a multimillennial climate model simulation with glacial CO_2 concentrations representative of Marine Isotope Stage 3. The Atlantic meridional overturning circulation (AMOC) and the subpolar gyre (SPG) oscillate on millennial time scales. When the AMOC is strong, the SPG is weak and contracted; when the AMOC is weak, the SPG is strong and extensive. The coupling between the two systems via wind-driven and density-driven feedbacks is key to maintaining the oscillations. The SPG controls the transport of heat and salt into the deep-water formation sites and thus controls the AMOC strength. The strength and location of the deep-water formation affect the density-driven part of the SPG and thus control the mean strength and extent of the SPG. This mechanism supports the hypothesis that coupled ocean-ice-atmosphere interactions could have triggered abrupt glacial climate change.

Plain Language Summary Between 57.000 and 29.000 years ago, the last glacial period was marked by several abrupt warming and cooling events over Greenland and the North Atlantic. Understanding the mechanism behind these so-called Dansgaard-Oeschger events increases our understanding of possible tipping points that cause abrupt change in the Earth system. The role of the ocean in causing these events is still a topic of debate. We find abrupt changes in the North Atlantic circulation that resemble Dansgaard-Oeschger events in a simulation with a state-of-the-art climate model. These simulated ocean circulation changes are generated without adding external triggers such as meltwater from glaciers. Instead, the events are generated by the interaction of the two large-scale current systems in the North Atlantic—the Atlantic meridional overturning circulation (AMOC) and the North Atlantic subpolar gyre (SPG). Both current systems are affected by changes in surface winds and the density pattern of the North Atlantic. We find that the location where the densest water is formed controls how the SPG interacts with the AMOC. Under favorable conditions, the effects of wind and density combine in such a way that changes in the SPG cause abrupt changes in the AMOC.

1. Introduction

The last glacial period featured abrupt climate transitions known as Dansgaard-Oeschger (D-O) events. These were especially frequent during Marine Isotope Stage 3 (MIS3), the period of 57 to 29 kyr before present. D-O events have been identified in Greenland ice cores as abrupt warming events followed typically by a more gradual cooling (e.g., Dansgaard et al., 1984; North Greenland Ice Core Project members, 2004; Oeschger et al., 1984). The impacts of D-O events are not limited to Greenland but can be traced over large parts of the globe in different proxy archives. A widely accepted hypothesis is that changes in the Atlantic meridional overturning circulation (AMOC) have played a key role in D-O events (e.g., Broecker et al., 1985; Clark et al., 2002; Rahmstorf, 2002). Reconstructions from marine sediment cores support this hypothesis (e.g., Henry et al., 2016; Lynch-Stieglitz, 2017). It is, however, still debated whether AMOC changes were the cause of D-O events or rather a reaction to externally forced abrupt climate change. Box model results and abrupt cooling or warming events in preindustrial control simulations point to changes in the North Atlantic subpolar gyre (SPG) as key to feedbacks that could generate D-O events without external forcing (e.g., Drijfhout et al., 2013; Kleppin et al., 2015; Li & Born, 2019). Identifying these feedbacks in glacial simulations would give further support to the GRL61418 hypothesis that D-O events could have occurred

unforced due to interactions between ocean, sea ice, and atmosphere in the North Atlantic. Even though there exist a few coupled climate simulations that produced D-O like, unforced AMOC oscillations in a cold, glacial-like climate (Brown & Galbraith, 2016; Klockmann et al., 2018; Peltier & Vettoretti, 2014), the role of the SPG in generating these oscillations has been largely neglected. Here, we analyze how AMOC and SPG interact during unforced AMOC transitions in a fully coupled simulation with MIS3-like atmospheric CO_2 concentrations.

The AMOC hypothesis is based on the idea that a strong ocean heat transport associated with a strong AMOC leads to warm conditions over the North Atlantic, while a weak ocean heat transport associated with a weak AMOC leads to cold conditions (e.g., Bryan, 1986; Clark et al., 2002; Manabe & Stouffer, 1988; Stocker & Wright, 1991). AMOC transitions could occur either externally forced or unforced due to internal feedbacks. Triggers for externally forced AMOC transitions include surface freshwater forcing (e.g., Cessi, 1994; Ganopolski & Rahmstorf, 2002) or gradual changes in ice sheet height or CO_2 concentrations (Zhang et al., 2014, 2017). Mechanisms for unforced AMOC transitions include deep decoupling (Marotzke, 1990; Weaver & Sarachik, 1991; Winton & Sarachik, 1993), salt oscillations (Peltier & Vettoretti, 2014), and thermohaline oscillations (Brown & Galbraith, 2016; Welander, 1982). Regardless of whether the simulated AMOC oscillations were externally forced or spontaneous, they were typically associated with large changes in sea ice cover and shifts in deep-water formation sites from the Nordic Seas during warm periods to south of Iceland during cold periods. This pattern is also supported by reconstructions (e.g., Dokken et al., 2013; Rasmussen & Thomsen, 2004).

To cause changes in deep convection and sea ice in the North Atlantic, the transport of salt and heat at higher latitudes is especially important. The oceanic transport of salt and heat in the Atlantic can be decomposed into contributions of the AMOC and the SPG. North of 45°N, the contribution of the SPG is stronger than that of the AMOC (e.g., Jungclaus et al., 2013). Therefore, changes in the SPG could also have the potential to trigger abrupt temperature changes. An abrupt weakening of the SPG likely played a key role in triggering the Little Ice Age (Moreno-Chamarro et al., 2016). Greenland temperature changes of D-O event magnitude were generated by stochastic wind forcing and resulting SPG changes in a preindustrial control simulation Kleppin et al. (2015). It is, however, likely, that D-O events were associated with changes in both the AMOC and SPG (Li & Born, 2019) because AMOC and SPG are tightly coupled on decadal to centennial time scales (e.g., Hátún et al., 2005; Thornalley et al., 2009; Yeager, 2015). The SPG is sensitive to both wind and buoyancy forcing (e.g., Born & Stocker, 2014; Levermann & Born, 2007; Montoya et al., 2011). Buoyancy forcing also affects deep-water formation in the North Atlantic, which in turn affects the AMOC strength.

Whether the correlation of the AMOC and SPG during D-O events was positive or negative is still an open question. A box model of the SPG and abrupt warming or cooling events in preindustrial control simulations indicated a positive feedback loop between wind forcing and deep convection in the Labrador Sea, that is, the *SPG center* (Li & Born, 2019). This mechanism suggests a positive correlation between the AMOC and SPG, and thus a strong SPG and AMOC during interstadials and a weak SPG and AMOC during stadials (Li & Born, 2019). However, if deep convection during MIS3 occurred instead mainly on the *SPG rim*, namely in the eastern North Atlantic and the Nordic Seas, the buoyancy forcing would reduce the cross-gyre density gradient and thus weaken the SPG (e.g., Montoya et al., 2011; Zhang et al., 2011). In that case, the correlation would have been negative with a weak SPG during interstadials and a strong SPG during stadials. In a simulation of the Last Glacial Maximum (LGM), the salt transport of the SPG played an important role in feeding a convective instability in the Irminger Sea, which triggered the transition from stadial to interstadial conditions (Vettoretti & Peltier, 2016, 2018). However, the authors of that study did not further investigate the correlation between AMOC and SPG. Here, we analyze the interaction of the AMOC and SPG during self-sustained AMOC oscillations that occur in a multimillennial climate simulation with MIS3-like CO_2 concentrations. We show that SPG dynamics are key to triggering the D-O like AMOC oscillations. We further show that wind-driven and density-driven feedbacks act at different periods of the AMOC oscillations and that the sign of the AMOC-SPG correlation depends on the dominant feedback and on the phase of the oscillation.

2. Simulation

We analyze a simulation with the Max Planck Institute Earth System Model (MPI-ESM) in which self-sustained, millennial-scale AMOC oscillations occur (Figure 1a). MPI-ESM is run in the
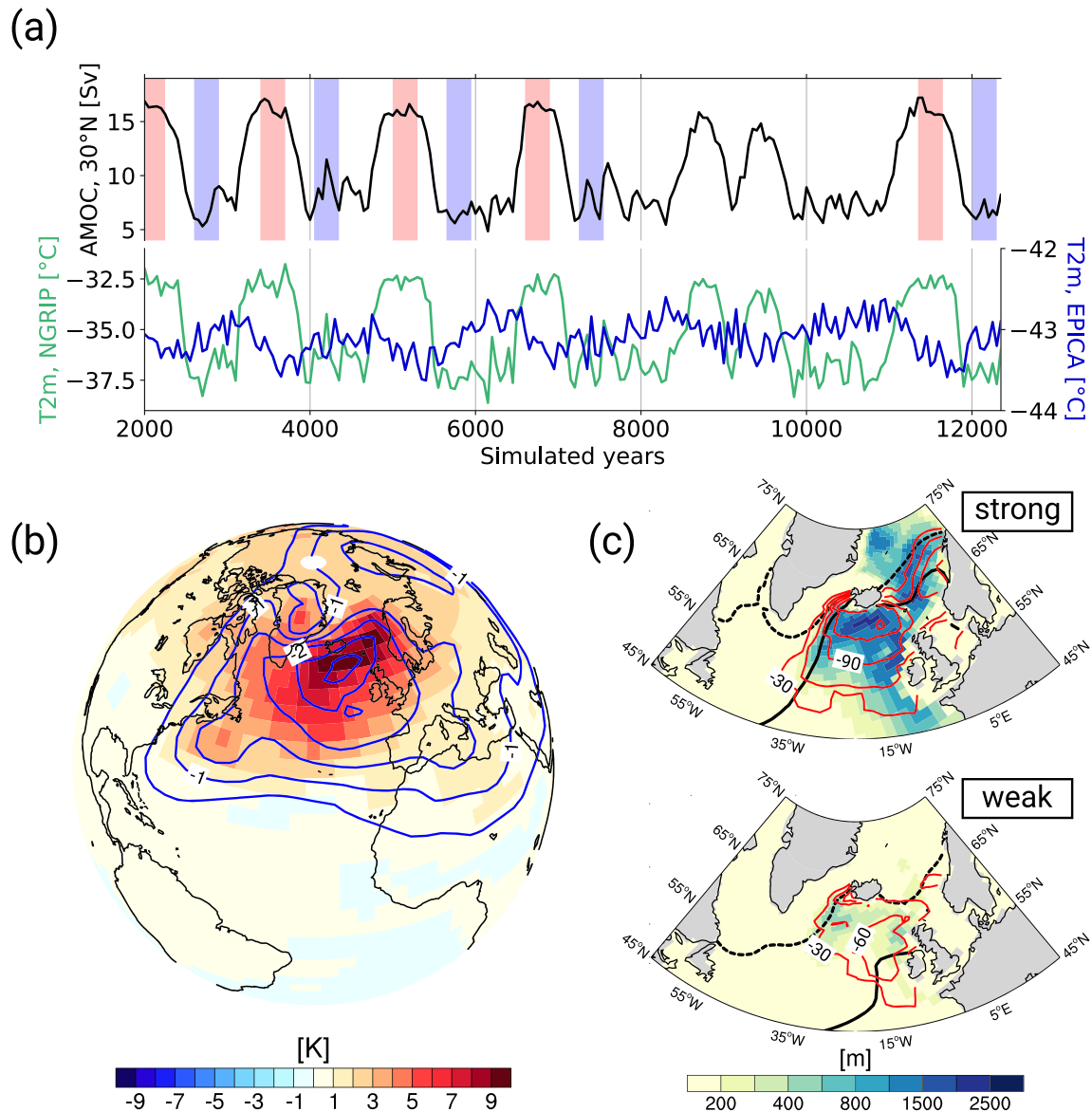
Figure 1. (a) Time series (50-year averages) of maximum AMOC strength at 30°N and 2 m air temperature in Greenland and Antarctica at the grid points closest to the NGRIP (green) and EPICA (blue) drilling sites, respectively. Red and blue bars mark the periods chosen for the strong and weak AMOC composites. (b) Composite difference (strong-weak) of 2 m air temperature (shading) and sea-level pressure (contours from −3.0 to −0.5 hPa in 0.5 hPa steps). (c) Composite mean mixed-layer depth (shading), net heat flux (red), and sea ice edge in summer (black dashed) and winter (black solid). The sea-ice edges are defined as the 30% contour of minimum and maximum sea ice cover.

coarse-resolution setup (T31/GR30). The curvilinear grid configuration with one grid pole over Greenland allows for a finer grid spacing of 50–100 km in the subpolar North Atlantic and a realistic simulation of deep convection. Further details are given by Klockmann et al. (2016) and Klockmann (2017).

The simulation is integrated for more than 12,000 years with constant forcing: preindustrial topography, ice sheets, and bathymetry, an atmospheric CO_2 concentration of 206 ppm and LGM orbital parameters. This simulation is the same as experiment "P206" in Klockmann et al. (2018, hereafter K18). The CO_2 concentration is a good approximation of MIS3 CO_2 concentrations which were approximately in the range of 200 to 220 ppm (e.g., Schilt et al., 2010). The prescribed ice sheets and the orbital configuration do not represent MIS3 conditions. This particular forcing combination favors AMOC oscillations in MPI-ESM because the AMOC is in a regime with two weakly unstable states (see K18 for details). Even though the forcing does not completely represent MIS3 conditions, the simulated AMOC oscillations resemble D-O events in many

aspects and present a good opportunity to investigate the interaction of the AMOC and SPG during D-O-like ocean circulation changes.

3. Millennial-Scale AMOC Oscillations and D-O Resemblance

The simulated AMOC oscillates between a weak and a strong state. The strong AMOC has a mean strength of 16 to 17 Sv; the strength of the weak AMOC varies between 5 to 11 Sv on centennial time scales (Figure 1a). The composite-mean difference between the weak and strong AMOC phases is 8.5 Sv, which agrees well with a stadial-interstadial AMOC difference of 9 ± 1.2 Sv reconstructed from AMOC-SST fingerprints (Zhang et al., 2015).

The simulated AMOC oscillations have a typical periodicity of 1,500 to 2,000 years. The strong phases last ∼500 to 700 years; the weak phases last 1,000 to 1,300 years. The Greenland ice core records indicated that the timing between warming events was not constant but ranged from ∼1,000 to 5,000 years (e.g., Buizert et al., 2015), likely depending on changing forcing such as ice sheet volume (e.g., Boers et al., 2018). The longer D-O interstadials in the ice core record featured a sawtooth shape with an abrupt warming, a gradual cooling, and an abrupt cooling period (e.g., Lohmann & Ditlevsen, 2019). Some of the shorter interstadials (e.g., events 4, 5.2, 6, 10, and 15) were more symmetric with a less pronounced gradual cooling period. Our simulated events are most similar to these shorter interstadials both in terms of duration and the evolution of Greenland temperatures.

The simulated near-surface air temperature over Greenland and the North Atlantic is in phase with the AMOC (Figure 1a). The largest air temperature changes occur over the North Atlantic colocated with the largest sea ice changes (Figure 1b, shading). Reconstructed temperature changes over Greenland are in the range of 10 ± 5 K (Kindler et al., 2014). At the grid point closest to the NGRIP location, the simulated temperature changes are at the lower end of the reconstructed range with 5 to 6 K (Figure 1a). With peak warming rates of 2.5 to 5 K/decade, the abrupt warming periods last ∼10 to 50 years. The abrupt cooling periods last between 70 and 170 years with cooling rates of 0.5 to 3.5 K/decade. The duration of the warming and cooling periods agrees well with reconstructions (Lohmann & Ditlevsen, 2019; Steffensen et al., 2008; Thomas et al., 2009). The simulated temperatures over Greenland and Antarctica (Figure 1a) show a bipolar seesaw effect (Stocker & Johnsen, 2003) in good agreement with ice core data (e.g., Blunier et al., 1998; Buizert et al., 2015).

Reconstructions and modeling studies indicated that large changes in sea ice cover occurred in the North Atlantic and the Nordic Seas during D-O events (e.g., Masson-Delmotte et al., 2005; Guillevic et al., 2013; Li et al., 2005, 2010; Sadatzki et al., 2019). During D-O stadials, the Nordic Seas were likely completely ice covered and without active deep convection. As a consequence, subsurface waters in the Nordic Seas were warmer during stadials than during interstadials because heat release to the atmosphere was limited (Dokken et al., 2013; Rasmussen & Thomsen, 2004). Similar changes in sea ice cover, deep convection, and subsurface temperatures occur in the Nordic Seas during the simulated AMOC transitions. During strong AMOC phases, the Nordic Seas are partly ice-free, and the eastern North Atlantic is completely ice-free (Figure 1c). Continuous deep convection occurs in the Irminger Sea, the Iceland basin and the Nordic Seas, indicated by composite-mean mixed-layer depths of 1,500 to 2,000 m and strong heat loss (Figure 1c). During weak AMOC phases, the Nordic Seas are completely ice covered. The subsurface water in the Nordic Seas is about 3 K warmer than during strong AMOC phases (not shown). Deep convection is confined to the Iceland basin and occurs only sporadically, indicated by the very shallow composite-mean mixed-layer depths (Figure 1c).

4. SPG Dynamics Control AMOC Transitions via Wind and Density Feedbacks

The AMOC transitions are tightly coupled to the strength and extent of the SPG. We use the barotropic stream function in the North Atlantic to describe the SPG (see also Text S1 in the supporting information). In the composite means, the two current systems are negatively correlated, that is, when the AMOC is weak, the SPG is strong and extensive; when the AMOC is strong, the SPG is weak and contracted (Figure 2, top panels). The state of the SPG has a strong effect on the salinity distribution in the North Atlantic. When the SPG is strong and extensive, the North Atlantic is dominated by fresh, subpolar water (Figure 2, top left), and the inflow of water from the subtropical gyre is limited to the very southeastern corner of the SPG. When the SPG is weak and contracted, the inflow of salty water from the subtropical gyre extends over the
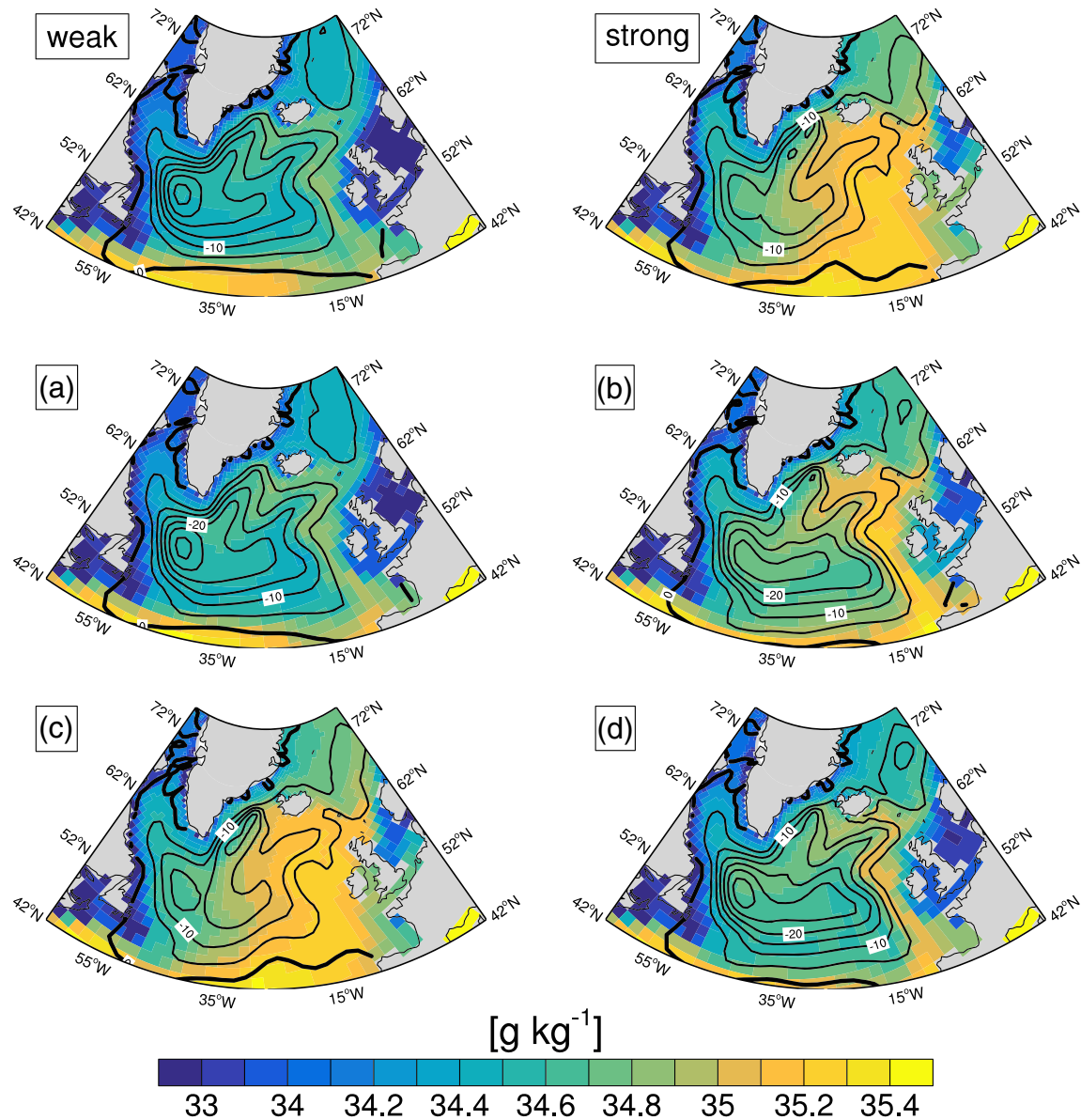
Figure 2. Salinity averaged over the upper 500 m (shading) and the barotropic stream function (contours, shown only for cyclonic rotation in intervals of 5 Sv). The upper two panels show composites for the weak and the strong AMOC phases; the lower four panels correspond to the periods marked by A, B, C, and D in Figure 3.

entire eastern half of the North Atlantic basin (Figure 2, top right). A similar relationship between the state of the SPG and the inflow of subtropical water was identified on decadal time scales since the 1960s (Hátún et al., 2005) and also on longer time scales during the Holocene (Thornalley et al., 2009). The coupling of the SPG and the AMOC can thus be explained by the role of the SPG in modulating the salt transport to the deep-water formation areas in the subpolar North Atlantic.

In the following, we investigate this coupling mechanism in detail and show that there are two distinct coupling regimes, depending on how wind and density forcing of the SPG interact. Since the eastern SPG seems to be key to modulating the inflow of subtropical water to the subpolar regions, we define an eastern SPG index (ESPGI) as the spatial average of the barotropic stream function in the eastern SPG (Figure 3g). The ESPGI captures changes in both the strength and extent of the eastern SPG. It also reflects the variability in the northeastern subtropical gyre as well as shifts in the boundary between both gyres (Figure S1). We analyze the transition cycle between simulation years 4,000 and 6,500; all other complete cycles show a similar behavior (Figure S2 and Text S2).
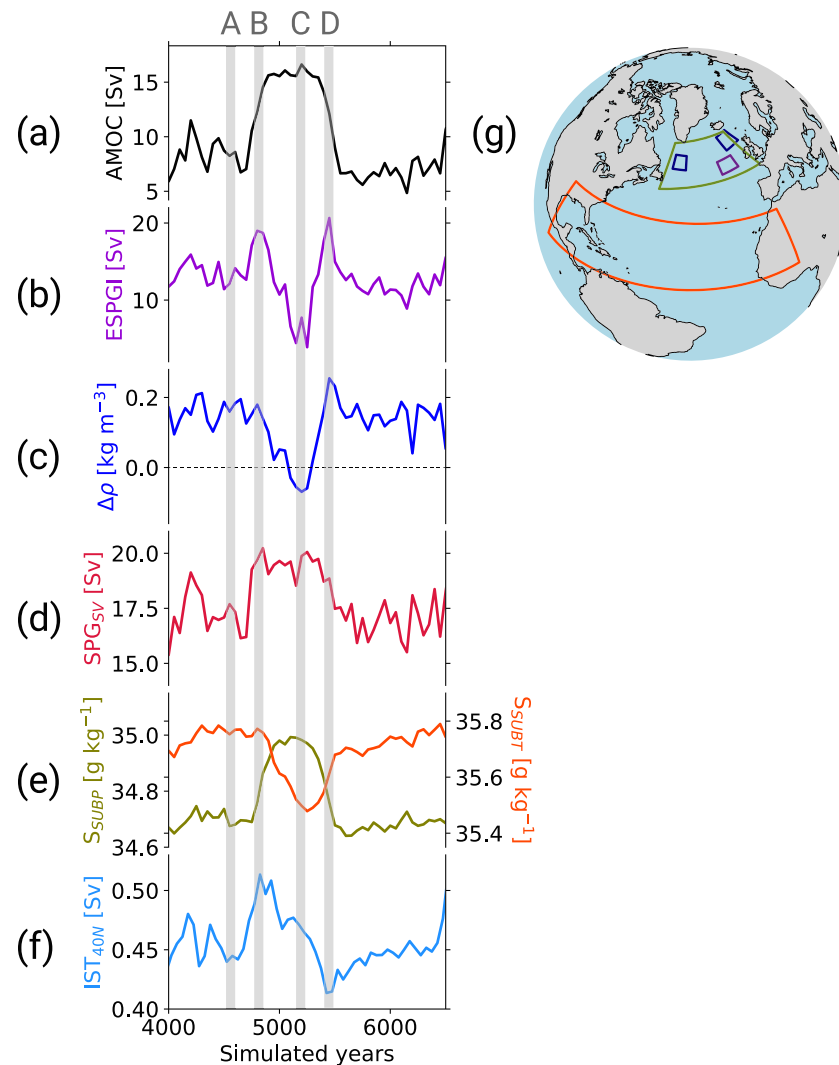
Figure 3. Time series (50-year averages) of (a) maximum AMOC strength at 30°N; (b) eastern SPG index, calculated as the mean of the barotropic stream function in the purple box in (g); (c) potential-density difference averaged over the upper 500 m between the center and the rim of the SPG (blue boxes in g). (d) The wind-driven SPG component, defined as the maximum Sverdrup transport in the subpolar North Atlantic; (e) salinity of the upper 1,000 m in the subtropical (orange) and subpolar (olive) North Atlantic (orange and olive box in g), respectively); (f) implied northward salt transport (IST) at 40°N, calculated as in Text S3 in the supporting information; (g) averaging areas.

4.1. Weak AMOC Phase

During the weak AMOC phase ("A," Figure 3), there is a core of dense water in the center of the SPG, and light water circulates along the rim (not shown). This leads to a large density difference between the center and the eastern rim of the SPG (Figure 3c). The wind-driven component of the SPG is relatively weak and accounts for only about 50% of the total SPG strength (Figures 3d and S3). The extensive North Atlantic sea ice cover leads to a weak Icelandic Low (not shown) and consequently to a weak wind stress curl and Sverdrup transport. But wind forcing may only be of secondary importance during this period because the sea ice partly decouples the surface ocean from the surface wind forcing (Jochum et al., 2012; Li & Born, 2019). Therefore, the cross-gyre density difference is likely the dominant driver of the SPG during the weak AMOC phase.

With the extensive SPG, the inflow of salty water from the subtropical to the subpolar North Atlantic ("A," Figures 2 and S4) is limited, and the northward salt transport is relatively low (Figure 3f). Salt accumulates slowly in the subtropics and the salinity difference between the subtropical and subpolar North Atlantic

is high (Figure 3e). The low northward salt transport is not sufficient to maintain active deep convection (cf. Figure 1c) and the AMOC remains weak.

4.2. AMOC Strengthening

The initial AMOC strengthening ("B," Figures 2 and 3) occurs simultaneously with an acceleration of eastern SPG (Figures 3a and 3b). The acceleration seen in the ESPGI cannot be explained by density forcing because the cross-gyre density difference remains on a similar level as before (Figure 3c). Instead, the acceleration is likely wind-driven and initiated by a feedback loop between sea ice cover and sea-level pressure (SLP). An initial—perhaps random—negative sea ice anomaly causes increased heat release to the atmosphere. The atmosphere warms and a negative SLP anomaly develops (cf. Figure 1b). This strengthens the Icelandic Low; the stronger southwesterly winds advect warmer air toward the sea ice edge and lead to a further retreat of the sea ice. The process could be described as the reverse of the cold-core high formation described by, for example, Drijfhout et al. (2013). The stronger Icelandic Low increases the wind stress curl, and the retreating sea ice increases the coupling of the surface wind forcing and the ocean circulation. As a result, the Sverdrup transport increases (Figure 3d) and the eastern SPG accelerates.

The accelerated eastern SPG leads to the AMOC strengthening: With the increased ESPGI, the northward salt transport increases ("B," Figure 3f). The high subtropical-subpolar salinity difference acts as a preconditioning for this peak in northward salt transport. The inflow of salty subtropical water is still limited to the very eastern flank of the SPG, but the acceleration leads to more entrainment of subtropical water into the SPG, and the salinity along the eastern SPG flank increases ("B," Figure 2). The increased supply of salt to the potential deep-water formation sites in the Iceland basin, Irminger Sea, and Nordic Seas triggers the onset of active deep convection and causes the AMOC strengthening.

4.3. Strong AMOC Phase

The continuous formation of dense water in the eastern North Atlantic and Nordic Seas changes the density pattern in the SPG region. The cross-gyre density difference decreases and ultimately reverses (from "Bt′" to "C," Figure 3c). At the same time, the ESPGI decreases rapidly (Figure 3b), reflecting both a weakening and a contraction of the SPG (compare "B" and "C," Figure 2). The Sverdrup transport during this period remains approximately constant; thus, the SPG weakening and contraction is driven by the changes in the cross-gyre density difference. This corresponds well to the simulated SPG response to a sudden onset of deep-convection in the Nordic Seas described by Montoya et al. (2011). While the cross-gyre density difference is reversed, the wind-driven SPG component accounts for the total maximum SPG strength (compare Figures S2 and S3).

During the weak and contracted SPG phase, the northward salt transport occurs via a broad inflow of subtropical water, which spans the entire eastern North Atlantic basin ("C," Figures 2 and S4). This way, the supply of salty water to the deep-convection sites remains very efficient, even though the subtropical salt content decreases (from "B" to "C," Figure 3e). Deep convection in the subpolar North Atlantic, and thus the strong AMOC, can only be maintained as long as the salinity difference between the subtropics and the subpolar regions is sufficiently high. The AMOC weakening is initiated when the subtropical salinity reaches its minimum ("C," Figure 3) and the subtropical-subpolar salinity difference becomes too small.

4.4. AMOC Weakening

The water that is now transported along the eastern SPG is fresher and lighter, which has several consequences: The cross-gyre density difference increases again (from "C" to "D," Figure 3c). The simultaneous rapid increase in the ESPGI reflects a density-driven acceleration and expansion of the SPG (compare "C" and "D," Figure 2). As the SPG expands, the flow at the southern gyre boundary becomes more zonal, and the inflow of subtropical water is again reduced to a very narrow band at the eastern flank of the SPG. The northward salt transport decreases rapidly. Even though the SPG accelerates again, the subtropical water that is entrained into the SPG is now warm and too fresh to sustain the deep convection in the eastern North Atlantic. Thus, the density-driven acceleration of the SPG helps to reestablish a halocline and triggers the AMOC weakening.

While deep convection and the AMOC weaken, sea ice expands again and heat release to the atmosphere is reduced. This cools the overlying atmosphere and induces a high-pressure anomaly, which weakens the Icelandic Low (not shown) and the wind stress curl over the North Atlantic. The SPG remains in its expanded

state but decelerates somewhat on its eastern flank ("D," Figures 2 and 3b) because the Sverdrup transport weakens ("D," Figure 3d), and the expanding sea ice decouples the surface ocean from the wind forcing. The weak AMOC phase is re-established: The strong SPG is maintained by a large cross-gyre density difference, the northward salt transport is very weak, and salinity accumulates in the subtropics.

4.5. Time Scales

The salinity changes and the basin-wide density adjustments also control the oscillation time scale. During the weak AMOC phase, the subtropical-salinity difference is on the order of $1\,\mathrm{g\,kg^{-1}}$. The initial salt transport into the Iceland basin due to the wind-driven spin up of the eastern SPG lasts about 15 to 20 years. The onset of deep convection on the SPG rim leads to a density-driven contraction of the SPG, which in turn enables an efficient salt transport to the eastern North Atlantic and Nordic Seas. This leads to a reduction in the subtropical-subpolar salinity difference on the order of $0.5\,\mathrm{g\,kg^{-1}}$ within 300 to 400 years. The duration of the strong AMOC phase is thus controlled by the erosion of the subtropical-subpolar salinity difference.

The AMOC weakening is initiated when the subtropical-subpolar salinity difference falls below a critical value of about $0.5\,\mathrm{g\,kg^{-1}}$. Deep convection cannot be sustained, the cross-gyre density difference begins to increase, and the density-driven acceleration and expansion of the SPG reduces the northward salt transport further. This leads to a rapid increase in the subtropical-subpolar salinity difference of about $0.5\,\mathrm{g\,kg^{-1}}$ within 200 to 250 years. The minimum duration of the weak AMOC phase is determined by the time it takes to recover the initial salinity difference through slow salt accumulation in the subtropics. The minimum duration is approximately 600 years during which the subtropical salt content increases by about $0.1\,\mathrm{g\,kg^{-1}}$. The total duration of the weak AMOC phase is controlled by the additional time it takes to reach favorable conditions for the wind-driven feedback to trigger the next AMOC increase. Reaching these conditions may require some stochasticity (Kleppin et al., 2015) which could explain why the duration of the weak phase is more variable than the duration of the strong phase.

5. Discussion and Conclusion

Our proposed mechanism for self-sustained AMOC-SPG oscillations combines three concepts: (1) salinity oscillations similar to Peltier and Vettoretti (2014), (2) a wind-driven feedback loop similar to Kleppin et al. (2015) and Drijfhout et al. (2013), and (3) a density-driven feedback loop similar to Montoya et al. (2011). Our results support the hypothesis of Li and Born (2019) that D-O events can be generated through oscillations in the coupled atmosphere sea-ice ocean system and that changes in the SPG are key to generating the oscillations. But while Li and Born (2019) suggest that the correlation between the SPG and the AMOC was positive for D-O events, we find that the correlation between the SPG and the AMOC depends on the dominant feedback and the phase of the oscillation. When the wind-driven feedback dominates, the correlation between the AMOC and the eastern SPG is positive (onset of AMOC strengthening); when the density-driven feedback dominates, the correlation between the AMOC and the entire SPG is negative (strong AMOC phase and onset of AMOC weakening).

The correlation between the AMOC and the SPG during D-O events is difficult to constrain by reconstructions as there are no available reconstructions of the SPG state during MIS3. Instead, proxy surrogate reconstructions (e.g., Jensen et al., 2018) could be a powerful tool to infer the state of the SPG from reconstructions of surface temperatures. Jensen et al. (2018) pointed out that their reconstruction was limited by a relatively small pool of simulations from which analog fields could be selected. But the simulation pool could be easily extended with the growing number of simulations in which unforced D-O like oscillations occur. Additionally, more detailed reconstructions of deep-water formation sites during MIS3 could help to infer the AMOC-SPG correlation because our results suggest that the location of the deep-water formation determines the sign of the density-driven feedback loop.

Indeed, one key difference between our results and those of Li and Born (2019) is the location of the deep-water formation. If the main deep-water formation is in the *center* of the SPG, that is, the Labrador and Irminger Sea, increased deep-water formation would increase the cross-gyre density difference and strengthen the SPG. This was the case in the box model of Li and Born (2019) and in the preindustrial control runs like Kleppin et al. (2015). But if the main deep-water formation is located in the eastern North Atlantic or the Nordic Seas—as is the case in our simulation—increased deep-water formation reduces the cross-gyre density difference and weakens the SPG. Comparing deep convection sites between models could

therefore help to understand differences in AMOC-SPG coupling. The evidence that deep convection was active in the Nordic Seas during interstadials and not active during stadials (Dokken et al., 2013; Rasmussen & Thomsen, 2004) suggests that the density structure in the North Atlantic may have undergone similar changes as in our simulation. Hence, we are confident that our simulation provides a plausible scenario for AMOC-SPG interactions during D-O events.

Conflict of Interest

The authors declare no conflict of interest.

Data Availability Statement

The model output used here is available at this site (https://cera-www.dkrz.de/WDCC/ui/cerasearch/entry?acronym=DKRZ_LTA_033_ds00002). The scripts for the analysis will be available online (https://hdl.handle.net/21.11116/0000-0004-87EE-8) upon publication.

References

Blunier, T., Chappellaz, J., Schwander, J., Dällenbach, A., Stauffer, B., Stocker, T. F., et al. (1998). Asynchrony of Antarctic and Greenland climate change during the last glacial period. *Nature*, *394*(6695), 739–743. https://doi.org/10.1038/29447

Boers, N., Ghil, M., & Rousseau, D.-D. (2018). Ocean circulation, ice shelf, and sea ice interactions explain Dansgaard–Oeschger cycles. *Proceedings of the National Academy of Sciences*, *115*(47), E11005–E11014. https://doi.org/10.1073/pnas.1802573115

Born, A., & Stocker, T. F. (2014). Two stable equilibria of the Atlantic subpolar gyre. *Journal of Physical Oceanography*, *44*(1), 246–264. https://doi.org/10.1175/JPO-D-13-073.1

Broecker, W. S., Peteet, D. M., & Rind, D. (1985). Does the ocean-atmosphere system have more than one stable mode of operation? *Nature*, *315*(6014), 21–26. https://doi.org/10.1038/315021a0

Brown, N., & Galbraith, E. D. (2016). Hosed vs. unhosed: Interruptions of the Atlantic meridional overturning circulation in a global coupled model, with and without freshwater forcing. *Climate of the Past*, *12*(8), 1663–1679. https://doi.org/10.5194/cp-12-1663-2016

Bryan, F. (1986). High-latitude salinity effects and interhemispheric thermohaline circulations. *Nature*, *323*(6086), 301–304. https://doi.org/10.1038/323301a0

Buizert, C., Adrian, B., Ahn, J., Albert, M., Alley, R. B., Baggenstos, D., et al. (2015). Precise interpolar phasing of abrupt climate change during the last ice age. *Nature*, *520*(7549), 661. https://doi.org/10.1038/nature14401

Cessi, P. (1994). A simple box model of stochastically forced thermohaline flow. *Journal of Physical Oceanography*, *24*(9), 1911–1920. https://doi.org/10.1175/1520-0485(1994)024<1911:ASBMOS>2.0.CO;2

Clark, P. U., Pisias, N. G., Stocker, T. F., & Weaver, A. J. (2002). The role of the thermohaline circulation in abrupt climate change. *Nature*, *415*(6874), 863–869. https://doi.org/10.1038/415863a

Dansgaard, W., Johnsen, S. J., Clausen, H. B., Dahl-Jensen, D., Gundestrup, N., Hammer, C. U., & Oeschger, H. (1984). North Atlantic climatic oscillations revealed by deep Greenland ice cores. *Climate Processes and Climate Sensitivity*, *29*, 288–298. https://doi.org/10.1029/GM029p0288

Dokken, T. M., Nisancioglu, K. H., Li, C., Battisti, D. S., & Kissel, C. (2013). Dansgaard-Oeschger cycles: Interactions between ocean and sea ice intrinsic to the Nordic Seas. *Paleoceanography*, *28*, 491–502. https://doi.org/10.1002/palo.20042

Drijfhout, S., Gleeson, E., Dijkstra, H. A., & Livina, V. (2013). Spontaneous abrupt climate change due to an atmospheric blocking–sea-ice–ocean feedback in an unforced climate model simulation. *Proceedings of the National Academy of Sciences*, *110*(49), 19,713–19,718. https://doi.org/10.1073/pnas.1304912110

Ganopolski, A., & Rahmstorf, S. (2002). Abrupt glacial climate changes due to stochastic resonance. *Physical Review Letters*, *88*(3), 038501. https://doi.org/10.1103/PhysRevLett.88.038501

Guillevic, M., Bazin, L., Landais, A., Kindler, P., Orsi, A., Masson-Delmotte, V., et al. (2013). Spatial gradients of temperature, accumulation and δ^{18}O-ice in Greenland over a series of Dansgaard–Oeschger events. *9*(3), 1029–1051. https://doi.org/10.5194/cp-9-1029-2013

Hátún, H., Sandø, A. B., Drange, H., Hansen, B., & Valdimarsson, H. (2005). Influence of the Atlantic subpolar gyre on the thermohaline circulation. *Science*, *309*(5742), 1841–1844. https://doi.org/10.1126/science.1114777

Henry, L. G., McManus, J. F., Curry, W. B., Roberts, N. L., Piotrowski, A. M., & Keigwin, L. D. (2016). North Atlantic ocean circulation and abrupt climate change during the last glaciation. *Science*, *353*(6298), 470–474. https://doi.org/10.1126/science.aaf5529

Jensen, M. F., Nummelin, A., Nielsen, S. B., Sadatzki, H., Sessford, E., Risebrobakken, B., et al. (2018). A spatiotemporal reconstruction of sea-surface temperatures in the North Atlantic during Dansgaard–Oeschger events 5–8. *Climate of the Past*, *14*(6), 901–922. https://doi.org/10.5194/cp-14-901-2018

Jochum, M., Jahn, A., Peacock, S., Bailey, D. A., Fasullo, J. T., Kay, J., et al. (2012). True to Milankovitch: Glacial inception in the new community climate system model. *Journal of Climate*, *25*(7), 2226–2239. https://doi.org/10.1175/JCLI-D-11-00044.1

Jungclaus, J. H., Fischer, N., Haak, H., Lohmann, K., Marotzke, J., Matei, D., et al. (2013). Characteristics of the ocean simulations in the Max Planck Institute Ocean Model (MPIOM) the ocean component of the MPI-Earth system model. *Journal of Advances in Modeling Earth Systems*, *5*, 422–446. https://doi.org/10.1002/jame.20023

Kindler, P., Guillevic, M., Baumgartner, M., Schwander, J., Landais, A., & Leuenberger, M. (2014). Temperature reconstruction from 10 to 120 kyr b2k from the NGRIP ice core. *Climate of the Past*, *10*(2), 887–902. https://doi.org/10.5194/cp-10-887-2014

Kleppin, H., Jochum, M., Otto-Bliesner, B., Shields, CA, & Yeager, S. (2015). Stochastic atmospheric forcing as a cause of Greenland climate transitions. *Journal of Climate*, *28*(19), 7741–7763. https://doi.org/10.1175/JCLI-D-14-00728.1

Klockmann, M. (2017). The AMOC and its sensitivity to different climate forcings in the range of glacial to modern conditions (Doctoral dissertation, Universität Hamburg). Berichte zur Erdsystemforschung. https://doi.org/10.17617/2.2472757

Klockmann, M., Mikolajewicz, U., & Marotzke, J. (2016). The effect of greenhouse gas concentrations and ice sheets on the glacial AMOC in a coupled climate model. *Climate of the Past*, *12*(9), 1829–1846. https://doi.org/10.5194/cp-12-1829-2016

Klockmann, M., Mikolajewicz, U., & Marotzke, J. (2018). Two AMOC states in response to decreasing greenhouse gas concentrations in the coupled climate model MPI-ESM. *Journal of Climate*, *31*(19). https://doi.org/10.1175/JCLI-D-17-0859.1

Levermann, A., & Born, A. (2007). Bistability of the Atlantic subpolar gyre in a coarse-resolution climate model. *Geophysical Research Letters*, *34*, L24605. https://doi.org/10.1029/2007GL031732

Li, C., Battisti, D. S., & Bitz, C. M. (2010). Can North Atlantic sea ice anomalies account for Dansgaard–Oeschger climate signals? *Journal of Climate*, *23*(20), 5457–5475. https://doi.org/10.1175/2010JCLI3409.1

Li, C., Battisti, D. S., Schrag, D. P., & Tziperman, E. (2005). Abrupt climate shifts in Greenland due to displacements of the sea ice edge. *Geophysical Research Letters*, *32*, L19702. https://doi.org/10.1029/2005GL023492

Li, C., & Born, A. (2019). Coupled atmosphere-ice-ocean dynamics in Dansgaard–Oeschger events. *Quaternary Science Reviews*, *203*, 1–20. https://doi.org/10.1016/j.quascirev.2018.10.031

Lohmann, J., & Ditlevsen, P. D. (2019). Objective extraction and analysis of statistical features of Dansgaard–Oeschger events. *Climate of the Past*, *15*(5), 1771–1792. https://doi.org/10.5194/cp-15-1771-2019

Lynch-Stieglitz, J. (2017). The Atlantic meridional overturning circulation and abrupt climate change. *Annual Review of Marine Science*, *9*, 83–104. https://doi.org/10.1146/annurev-marine-010816-060415

Manabe, S., & Stouffer, R. J. (1988). Two stable equilibria of a coupled ocean-atmosphere model. *Journal of Climate*, *1*(9), 841–866. https://doi.org/10.1175/1520-0442(1988)001<0841:TSEOAC>2.0.CO;2

Marotzke, J. (1990). Instabilities and multiple equilibria of the thermohaline circulation (Doctoral dissertation, Christian-Albrechts-Universität Kiel). Berichte des Instituts für Meereskunde Kiel. https://doi.org/10.3289/ifm_ber_194

Masson-Delmotte, V., Jouzel, J., Landais, A., Stievenard, M., Johnsen, S. J., White, J. W. C., et al. (2005). GRIP deuterium excess reveals rapid and orbital-scale changes in Greenland moisture origin. *Science*, *309*(5731), 118–121. https://doi.org/10.1126/science.1108575

Montoya, M., Born, A., & Levermann, A. (2011). Reversed North Atlantic gyre dynamics in present and glacial climates. *Climate Dynamics*, *36*(5–6), 1107–1118. https://doi.org/10.1007/s00382-009-0729-y

Moreno-Chamarro, E., Zanchettin, D., Lohmann, K., & Jungclaus, J. H. (2016). An abrupt weakening of the subpolar gyre as trigger of Little Ice Age-type episodes. *Climate Dynamics*, *48*, 727–744. https://doi.org/10.1007/s00382-016-3106-7

North Greenland Ice Core Project members (2004). High resolution record of Northern Hemisphere climate extending into the last interglacial period. *Nature*, *431*(7005), 147–151. https://doi.org/10.1038/nature02805

Oeschger, H., Beer, J., Siegenthaler, U., Stauffer, B., Dansgaard, W., & Langway, C. C. (1984). *Late glacial climate history from ice cores*. https://doi.org/10.1029/GM029p0299

Peltier, W. R., & Vettoretti, G. (2014). Dansgaard-Oeschger oscillations predicted in a comprehensive model of glacial climate: A kicked salt oscillator in the Atlantic. *Geophysical Research Letters*, *41*, 7306–7313. https://doi.org/10.1002/2014GL061413

Rahmstorf, S. (2002). Ocean circulation and climate during the past 120,000 years. *Nature*, *419*(6903), 207–214. https://doi.org/10.1038/nature01090

Rasmussen, T. L., & Thomsen, E. (2004). The role of the North Atlantic Drift in the millennial timescale glacial climate fluctuations. *Palaeogeography, Palaeoclimatology, Palaeoecology*, *210*(1), 101–116. https://doi.org/10.1016/j.palaeo.2004.04.005

Sadatzki, H., Dokken, T. M., Berben, S. M. P., Muschitiello, F., Stein, R., Fahl, K., et al. (2019). Sea ice variability in the southern Norwegian Sea during glacial Dansgaard-Oeschger climate cycles. *Science advances*, *5*(3), eaau6174. https://doi.org/10.1126/sciadv.aau6174

Schilt, A., Baumgartner, M., Schwander, J., Buiron, D., Capron, E., Chappellaz, J., et al. (2010). Atmospheric nitrous oxide during the last 140,000 years. *Earth and Planetary Science Letters*, *300*(1–2), 33–43. https://doi.org/10.1016/j.epsl.2010.09.027

Steffensen, J. P., Andersen, K. K., Bigler, M., Clausen, H. B., Dahl-Jensen, D., Fischer, H., et al. (2008). High-resolution Greenland ice core data show abrupt climate change happens in few years. *Science*, *321*(5889), 680–684. https://doi.org/10.1126/science.1157707

Stocker, T. F., & Johnsen, S. J. (2003). A minimum thermodynamic model for the bipolar seesaw. *Paleoceanography*, *18*(4), 1087. https://doi.org/10.1029/2003PA000920

Stocker, T. F., & Wright, D. G. (1991). Rapid transitions of the ocean's deep circulation induced by changes in surface water fluxes. *Nature*, *351*(6329), 729–732. https://doi.org/10.1038/351729a0

Thomas, E. R., Wolff, E. W., Mulvaney, R., Johnsen, S. J., Steffensen, J. P., & Arrowsmith, C. (2009). Anatomy of a Dansgaard-Oeschger warming transition: High-resolution analysis of the North Greenland ice core project ice core. *Journal of Geophysical Research*, *114*, D08102. https://doi.org/10.1029/2008JD011215

Thornalley, D. J. R., Elderfield, H., & McCave, I. N. (2009). Holocene oscillations in temperature and salinity of the surface subpolar North Atlantic. *Nature*, *457*(7230), 711–714. https://doi.org/10.1038/nature07717

Vettoretti, G., & Peltier, W. R. (2016). Thermohaline instability and the formation of glacial North Atlantic super polynyas at the onset of Dansgaard–Oeschger warming events. *Geophysical Research Letters*, *43*, 5336–5344. https://doi.org/10.1002/2016GL068891

Vettoretti, G., & Peltier, W. R. (2018). Fast physics and slow physics in the nonlinear Dansgaard–Oeschger relaxation oscillation. *Journal of Climate*, *31*(9), 3423–3449. https://doi.org/10.1175/JCLI-D-17-0559.1

Weaver, A. J., & Sarachik, E. S. (1991). The role of mixed boundary conditions in numerical models of the ocean's climate. *Journal of Physical Oceanography*, *21*(9), 1470–1493. https://doi.org/10.1175/1520-0485(1991)021<1470:TROMBC>2.0.CO;2

Welander, P. (1982). A simple heat-salt oscillator. *Dynamics of Atmospheres and Oceans*, *6*(4), 233–242. https://doi.org/10.1016/0377-0265(82)90030-6

Winton, M., & Sarachik, E. S. (1993). Thermohaline oscillations induced by strong steady salinity forcing of ocean general circulation models. *Journal of Physical Oceanography*, *23*(7), 1389–1410. https://doi.org/10.1175/1520-0485(1993)023<1389:TOIBSS>2.0.CO;2

Yeager, S. (2015). Topographic coupling of the Atlantic overturning and gyre circulations. *Journal of Physical Oceanography*, *45*(5), 1258–1284. https://doi.org/10.1175/JPO-D-14-0100.1

Zhang, R., Delworth, T. L., Rosati, A., Anderson, W. G., Dixon, K. W., Lee, H.-C., & Zeng, F. (2011). Sensitivity of the North Atlantic ocean circulation to an abrupt change in the Nordic Sea overflow in a high resolution global coupled climate model. *Journal of Geophysical Research*, *116*, C12024. https://doi.org/10.1029/2011JC007240

Zhang, X., Knorr, G., Lohmann, G., & Barker, S. (2017). Abrupt North Atlantic circulation changes in response to gradual CO_2 forcing in a glacial climate state. *Nature Geoscience*, *10*(7), 518–523. https://doi.org/10.1038/NGEO2974

Zhang, X., Lohmann, G., Knorr, G., & Purcell, C. (2014). Abrupt glacial climate shifts controlled by ice sheet changes. *Nature*, *512*, 290–294. https://doi.org/10.1038/nature13592

Zhang, X., Prange, M., Merkel, U., & Schulz, M. (2015). Spatial fingerprint and magnitude of changes in the Atlantic meridional overturning circulation during Marine Isotope Stage 3. *Geophysical Research Letters*, *42*, 1903–1911. https://doi.org/10.1002/2014GL063003